A preliminary study on the effects of cracks on chloride penetration in different concretes

N. Russo[1], M. Gastaldi[2], P. Marras[3], L. Schiavi[4], A. Strini[5] and F. Lollini[6]

ABSTRACT: The penetration of chloride ions into concrete is one of the most detrimental processes affecting durability of reinforced concrete (RC) structures. Concurrently, cracks are almost inevitable in RC constructions, providing an easy access to chlorides and therefore an accelerated reinforcement corrosion. In this paper preliminary results are presented, concerning the resistance to chloride penetration of different cracked and uncracked concretes - evaluated in terms of chloride migration coefficient – measured with non-steady state migration test. Sound and cracked prismatic specimens, realized with different cement types and a w/c ratio of 0.45, were tested. A specific cracking procedure was developed to obtain load-induced micro-cracks, characterized by a width ranging between 10 μm and 50 μm. Results showed that in correspondence of the micro-crack, the chloride migration coefficient was subjected to a local increase up to 2.2 times the value measured on sound concrete.

1 INTRODUCTION

Chloride-induced corrosion of steel rebar is one of the most widespread causes of structural failure in chloride-bearing environment (Bertolini *et al.*, 2007). The durability design in such environmental conditions – typically, in marine environment or in presence of de-icing salts – is a challenging task. Designers need reliable models to correctly assess the evolution of the deterioration process, based on several durability design parameters. Among others, chloride penetration resistance of concrete is of major concern. Models provide for its evaluation, in terms of chloride diffusion coefficient, and, through correlation coefficients, an estimation of the long-time behaviour of the material in real exposure conditions (*fib* Model Code for Service Life Design, 2006). However, models refer mainly to uncracked concrete, a condition that rarely occurs in practice. Cracks are almost inevitable, due to several physical phenomena – such as thermal gradients, freeze-thaw cycles, shrinkage and mechanical loading – and appear since the very beginning of the life of a structure. They generate discontinuity in the concrete cover thickness, accelerating the penetration of detrimental substances.

In recent years, several studies have been carried out to evaluate the effects of cracks on chloride ions penetration in concrete. The research activity on this topic, however, is characterized by a great heterogeneity, and therefore it is difficult to compare results obtained in different studies. As a general result, it seems that crack width at the exposed surface is a key parameter influencing chloride penetration resistance of cracked concrete. Several studies have been addressed in finding the value of critical crack width (w_{cr}) intended as the minimum crack width at concrete surface causing an increase in chloride diffusion coefficient with respect to uncracked concrete. Results show that w_{cr} is mainly included in the range of micro-cracks (width smaller than 100 μm) far below the maximum allowable values considered in current regulations and technical committee for structural design in severe environments, which is for instance 330 μm according to ACI committee 318, 1999.

[1] *Ph.D. student, Politecnico di Milano, CMIC Dept. "Giulio Natta", nicoletta.russo@polimi.it*
[2] *Assistant professor, Politecnico di Milano, CMIC Dept. "Giulio Natta", matteo.gastaldi@polimi.it*
[3] *Research Technician, CNR, Istituto per le Tecnologie della Costruzione, pietro.marras@itc.cnr.it*
[4] *Researcher, CNR, Istituto per le Tecnologie della Costruzione, luca.schiavi@itc.cnr.it*
[5] *Researcher, CNR, Istituto per le Tecnologie della Costruzione, alberto.strini@itc.cnr.it*
[6] *Assistant professor, Politecnico di Milano, CMIC Dept. "Giulio Natta", federica.lollini@polimi.it*

Furthermore, w_{cr} reported in literature are strictly related to the adopted experimental procedure. Considering only fully saturated conditions, the chloride ions penetrate in concrete mainly due to diffusion, a low-penetration-rate mass transport phenomenon. The values of w_{cr} evaluated through conventional diffusion test methods are included in the range between 30 μm (Ismail *et al.*, 2008) and 135 μm (Şahmaran, 2007). In order to accelerate the penetration of chlorides, in recent years, an increasing number of studies has employed accelerated laboratory tests. The cracking procedure most frequently used in these cases has been the feedback-controlled splitting test, generating tensile-induced cracks with controlled mouth opening displacement. Different typologies of accelerated test methods have been used to evaluate an overall chloride diffusion coefficient of cracked concrete, and subsequently the coefficient in correspondence of crack has been analytically derived (Djerbi *et al.*, 2008, Jang *et al.*, 2011, Park *et al.*, 2012). With this procedure, w_{cr} resulted to be around 80 μm (Jang *et al.*, 2011). As an alternative, several researchers have adopted the so-called Rapid Chloride Migration (RCM) test, that is associated to a colorimetric technique for the detection of chloride penetration profile, even in the proximity of cracks. Nevertheless, this experimental procedure has been mostly associated with the realization of artificial cracks, named notches, characterized by smooth and parallel walls and wide widths, rarely included in the range of micro-cracks (Audenaert *et al.*, 2007, Marsavina *et al.*, 2009, Li *et al.*, 2016). Under the same exposure conditions, geometrical features of artificial notches have shown to have a significant influence on the value of critical crack width, if compared to load-induced cracks. With regard to RCM test, in a study with artificial notches w_{cr} resulted to be 50 μm (Li *et al.*, 2016) while for load-induced cracks w_{cr} resulted to be 13 μm (Yoon and Schlangen, 2014).

A further issue is related to the influence of different concrete types. In Jang *et al.*, 2011, has been reported that the addition of fly ash has resulted in lower values of diffusion coefficient with a similar trend as in uncracked concrete. On the contrary, in a study based on wide artificial cracks, the addition of fly ash have resulted in almost identical penetration profiles with respect to ordinary Portland concrete, while the addition of silica fume produced a lower penetration depth and a steeper chloride penetration profile (Sosdean *et al.*, 2016).

In summary, it is still not completely clear how durability design parameters are influenced by the presence and the geometrical features of cracks, and for this reason the research activity on the subject is still in progress.

In this study preliminary results are presented, as part of a wider project concerning the evaluation of chloride penetration resistance of sound and cracked concrete. RCM test was carried out on uncracked and load-induced cracked concrete, made with four different cement types, w/c ratio of 0.45, and considering two different times of curing.

2 EXPERIMENTAL PROCEDURE

2.1 Materials and Methods

Four different concrete mixes were investigated, as listed in Table 1. A preliminary analysis, aimed at investigating the possibility of performing RCM test on prismatic specimens, was carried out on a Portland-Limestone cement (P-PLC), type CEM II/B-LL 42,5R according to UNI EN 197-1. Afterwards, Ordinary Portland Cement (OPC) type CEM I 42,5R, a Portland-Limestone cement (PLC) type CEM II/A-LL 42,5R, and a Pozzolanic Cement (PC) type CEM IV/A(V) 42,5R-SR were used. All the concrete mixes were manufactured with 422 kg/m^3 of cement, 190 kg/m^3 of water (w/c ratio equal to 0.45), and 1731 kg/m^3 of calcareous aggregates, subdivided into five grain size fractions with a maximum diameter of 9 mm. An acrylic-based superplasticizer was also added to the mix, to improve workability. Details on slump are reported in Table 1, except those referred to P-PLC that was not characterized at fresh and hardened state.

For P-PLC a single batch of concrete mix was realised to obtain four cylindrical specimens and four prismatic specimens. The former ones were characterized by a thickness

of 50 mm and a diameter of 100 mm. Two of them were individually cast in cylindrical PVC moulds (cast surface will be exposed to chlorides), while the other two were sliced from a 150 mm high cylinder (cut surface will be exposed to chlorides). The prismatic specimens had dimensions of 120×90×50 mm and were individually cast in PVC moulds. Two of them were provided with a V-shaped notch in the longitudinal direction on the casting surface. The notch was around 5 mm deep, and promoted the formation of the longitudinal crack as the specimen was subjected to the cracking procedure (section 2.2).

Table 1. Details on concrete mixing proportions and properties.

	P-PLC	*OPC*	*PLC*	*PC*
Cement, kg/m^3	*422*	*422*	*422*	*422*
Water, kg/m^3	*190*	*190*	*190*	*190*
Aggregate, kg/m^3	*1731*	*1731*	*1731*	*1731*
w/c ratio	*0.45*	*0.45*	*0.45*	*0.45*
Slump, mm	-	*140*	*148*	*55*
Density, kg/m^3	-	*2451*	*2494*	*2494*
$f_{c,cube,28days}$, MPa	-	*76.3*	*63.3*	*68.5*

As it concerns the other concrete types, a single batch was realized for each mix design, to obtain two cubic specimens, 100 mm side, and eight prismatic specimens. Prismatic specimens had the same dimensions and were manufactured with the same procedure of previous P-PLC specimens. For each concrete type, four specimens were provided with the longitudinal notch, and subsequently subjected to the cracking procedure. After casting, the specimens were covered with a plastic film, and one day after casting, were demoulded and kept in the curing tank, at 20°C and RH>90%.

Cylindrical and prismatic specimens made with P-PLC were cured for 7 days in moist conditions. For the other concretes two sound and two cracked specimens were cured in moist conditions for 7 days, whilst two sound and two cracked specimens and the cubes for 28 days. Compressive strength test was performed according to UNI EN 12390-3 standard on cubic specimens, while RCM test (Section 2.3) was performed on prismatic and cylindrical specimens.

In the following sections, to refer to the type of concrete considered, the same codes reported in Table 1 will be used, followed by the number identifying the days of curing (e.g. PLC-7 refers to Portland-limestone cement tested after 7 days of curing).

2.2 Cracking procedure

A specific cracking method was developed in order to obtain load-induced, V-shaped cracks on the casting surface, as it could occur in real structures. The day after casting, prismatic specimens with longitudinal notch were demoulded, enclosed within a steel confinement system, and placed in a universal testing machine, with the notch facing downwards. Two rubber strips, 15 mm wide, were positioned on the two sides of the longitudinal notch, at a distance of 30 mm, and one (30 mm wide) at the centre on the upward face, in a three-point bending test configuration (Figure 1). The specimen is loaded applying a 0.5 mm/min strain to the upward central rubber strip. The first appearance of crack was visually detected. The value of load corresponding to this point was then increased of a 20% of overload (several tests had been made to define the value of overload and the position of the rubber strips, in order to obtain acceptable cracks). Once the overload was reached, the load was released and the confinement system was removed from the specimen. The geometrical features of cracks obtained with this specific cracking procedure will be reported in section 3.1.

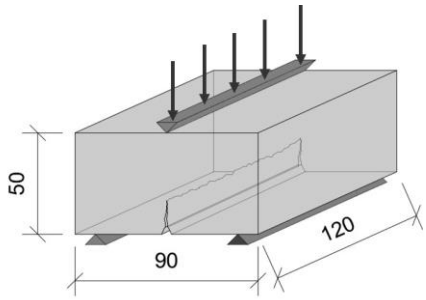

Figure 1. Specimen geometry and cracking procedure (dimension in mm).

2.3 Resistance to chloride penetration

Chloride penetration resistance of concrete was evaluated with non-steady state migration test, in accordance with NT BUILD 492 (Nordtest method NT BUILD 492, 1999). After the curing, the specimens were vacuum saturated in $Ca(OH)_2$ solution. Then cylindrical specimens were mounted in rubber sleeves and stainless steel clamps to ensure water tightness of curved, lateral surfaces. On the other hand, preparation of the prismatic specimens was slightly modified in order to adapt to the different sample geometry. At the end of the saturation procedure each specimen was fit in a rigid PVC four-walls box. The junction between PVC walls and the concrete specimen and the junction between different PVC walls was sealed. To further ensure water tightness, ratchet straps were externally wrapped and tightened. Moreover, PVC walls were designed to create a container for the anolyte solution. After being mounted, the specimens were placed on a plastic support with 30° of inclination, the upward face was exposed to the anolyte solution (0.3 M NaOH), while the downward face (corresponding to cast surface) to the catholyte solution, 10% NaCl (Figure 2). An initial pre-set voltage of 30 V was supplied, recording the electrical current flowing in the system. Based on this value, an adjustment of the applied voltage was always necessary, following the method prescriptions, and duration of the test was determined (24 hours for all the specimens).

Once the test was concluded, the samples were split. For prismatic specimens, the split was executed in two different points along the longitudinal direction, i.e. for cracked specimens the splitting surface was perpendicular to the crack plane. Colorimetric technique was used to evaluate chloride penetration depth, spraying a silver nitrate solution (0.1 M) on the freshly split surfaces (four for prismatic specimens, two for cylindrical ones) and chloride penetration depth was measured. On the freshly split surface, the measures were done in the central point, i.e. in correspondence of the symmetry axis of the surface, and on three further points on each side, at 10, 20 and 30 mm from central axis, being a total of seven measurement points. For cracked specimens the penetration depth in the central point was measured starting from the tip of the notch. Since the crack was not always perpendicular to the exposed surface, for cracked specimens an additional point was taken into account, in correspondence of the maximum chloride penetration depth. In this case, the distance with respect to the central axis of the section and the penetration depth from the tip of the notch were measured.

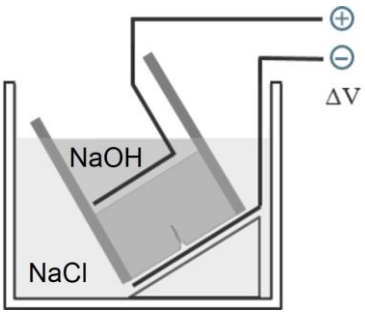

Figure 2. Rapid chloride migration testing procedure.

From the measurements of penetration depths, the non-steady-state migration coefficient (D_{RCM}) was evaluated as:

$$D_{RCM} = \frac{RT}{zFE} \cdot \frac{x - \alpha\sqrt{x}}{t} \qquad (1)$$

Where R is the gas constant (8.314 J/K mol), T is the average value of the temperatures in the anolyte solution (K), z is the absolute value of ion valence (for chloride z=1), F is the Faraday constant (9.648×10^4 J/V mol), t is test duration (s), x is the penetration depths (m), E=(U-2)/L (where U is the applied voltage in V and L is the thickness of the specimen in m), and α is calculated as:

$$\alpha = 2\sqrt{\frac{RT}{zFE}} erf^{-1}\left(1 - \frac{2c_d}{c_0}\right) \qquad (2)$$

Where c_d is the chloride concentration corresponding to the colour change (≈ 0.07 N for Portland cement concrete) and c_o is the chloride concentration (≈ 2N) in the catholyte solution (Nordtest method NT BUILD 492, 1999).

The geometrical features of cracks were observed at the end of the RCM test. A superfluid two-component epoxy resin was poured on one of the split surfaces of each specimen. After 24 hours a very thin slice parallel to the split surface was sawed with a water cooled cutting saw. The two cut surfaces were then polished, and observed with a stereomicroscope. The aim was to measure crack parameters such as crack opening at the exposed surface and crack depth, in correspondence of the split surface.

3 RESULTS AND DISCUSSION

3.1 Characterization of cracks

Figure 3 reports, as an example, two images obtained at 50x of magnification, for one of the OPC-28 cracked specimens. Surface width was clearly measurable in correspondence of notch (Figure 3a) and crack path was clearly detectable until crack tip, corresponding to a crack width of about 15 μm (Figure 3b). For each cutting surface crack tip was identified, and crack depth was measured as the distance between this point and notch tip. The relationship between crack depth and crack surface width (henceforth simply called crack width) for all the tested specimens is reported in Figure 4. Crack widths were always included in the range between 10 and 50 μm (micro-cracks), while crack depths resulted up to 25 mm.

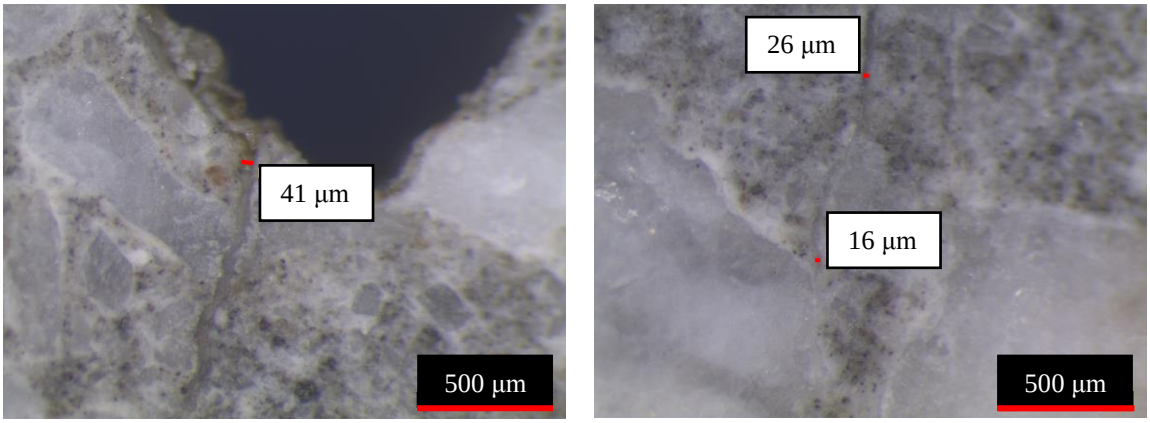

(a) *(b)*

Figure 3. Microscope images of cracked OPC-28 specimen referring to (a) crack width and (b) crack tip.

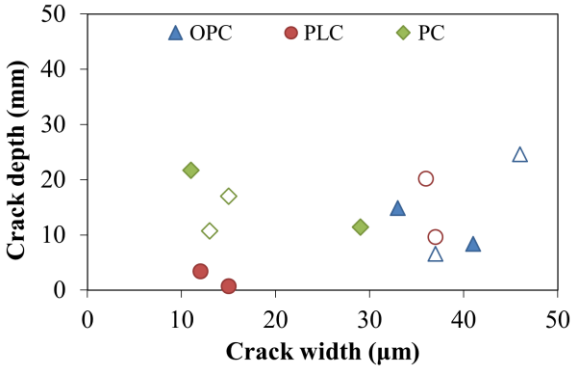

Figure 4. Crack width as a function of crack depth, (empty symbols represent 7-day cured specimens, filled symbols 28-day cured specimens).

Cracks obtained in this study were not induced by a width-controlled cracking procedure, and results showed that crack widths obtained for different concrete types were quite heterogeneous. In particular, very low values were obtained for PLC and PC concrete types. Considering the effect of curing time, for each concrete type the values of crack width for specimens tested after 7 days and after 28 days were quite consistent, except for PLC type. One possible explanation for these results could be self-healing, occurred in the crack during the curing time. However, according to Şahmaran, 2007 and Yoon and Schlangen, 2014, self-healing was observed to occur in cracks only for long-term exposure times. Future research will be carried out to investigate the topic.

3.2 Validation of experimental procedure

The investigation on P-PLC concrete type provided validation of the experimental procedure adopted in this work, NT BUILD 492. Two main variants were introduced, with respect to the procedure outlined in the standard: the characteristics of the surface exposed to chlorides, and the geometry of the specimen.

Figure 5 shows the values of D_{RCM} obtained on sound cylindrical specimens, both when cut and cast surfaces were exposed to chlorides, and on prismatic specimens. As expected, D_{RCM} for cast cylinders was higher with respect to cut cylinders, showing an increase of about 20%. Due to the bleeding effect, the physical properties of concrete in proximity of the casting surface can significantly differ from the inner concrete, leading to a more porous and permeable microstructure. As it concerns specimen geometry, the results obtained with cast cylinders and prismatic specimens are very similar, with values of D_{RCM} equal to 25.4×10^{-12} m^2/s and 23.7×10^{-12} m^2/s respectively.

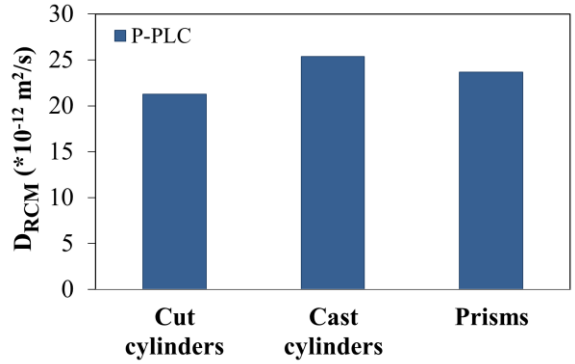

Figure 5. Non-steady-state migration coefficient for sound P-PLC concrete specimens.

This result was considered as a validation of the experimental procedure adopted in this work.

The prismatic geometry allows to enable a specific cracking procedure based on the three-point bending method. The aim is to realize concrete specimens with realistic, load-induced and V-shaped micro-cracks, suitable for the RCM test. After being validated, the testing procedure proposed in this study was applied on sound and cracked concrete specimens, made with the three different types of concrete. The RCM test was executed also on preliminary P-PLC cracked specimens. The chloride penetration depth, however, reached the whole specimen thickness in correspondence of cracks. For this reason, it was not possible to evaluate the D_{RCM} in correspondence of crack, and these results will not be reported in the next paragraph.

3.3 Resistance to chloride penetration

Chloride penetration resistance of each concrete type was analysed starting from the chloride penetration profiles. Figure 6 shows, as an example, the results in terms of penetration depths measured on OPC-7 and OPC-28 concrete specimens. In particular, Figures 6a and 6c show the penetration depths obtained at several measurement points of the eight different splitting surfaces (four splitting surfaces for both two sound specimens, and four splitting surfaces for the two cracked ones). It can be observed that the measurements carried out on sound specimens were quite uniform on the split surfaces if compared to measurements on cracked specimens. For cracked specimens, in fact, the chloride penetration depths far from the crack were similar to those obtained in sound concrete, while they increase approaching a maximum value in proximity of the crack. The measured penetration depths were then used to evaluate the non-steady-state migration coefficient.

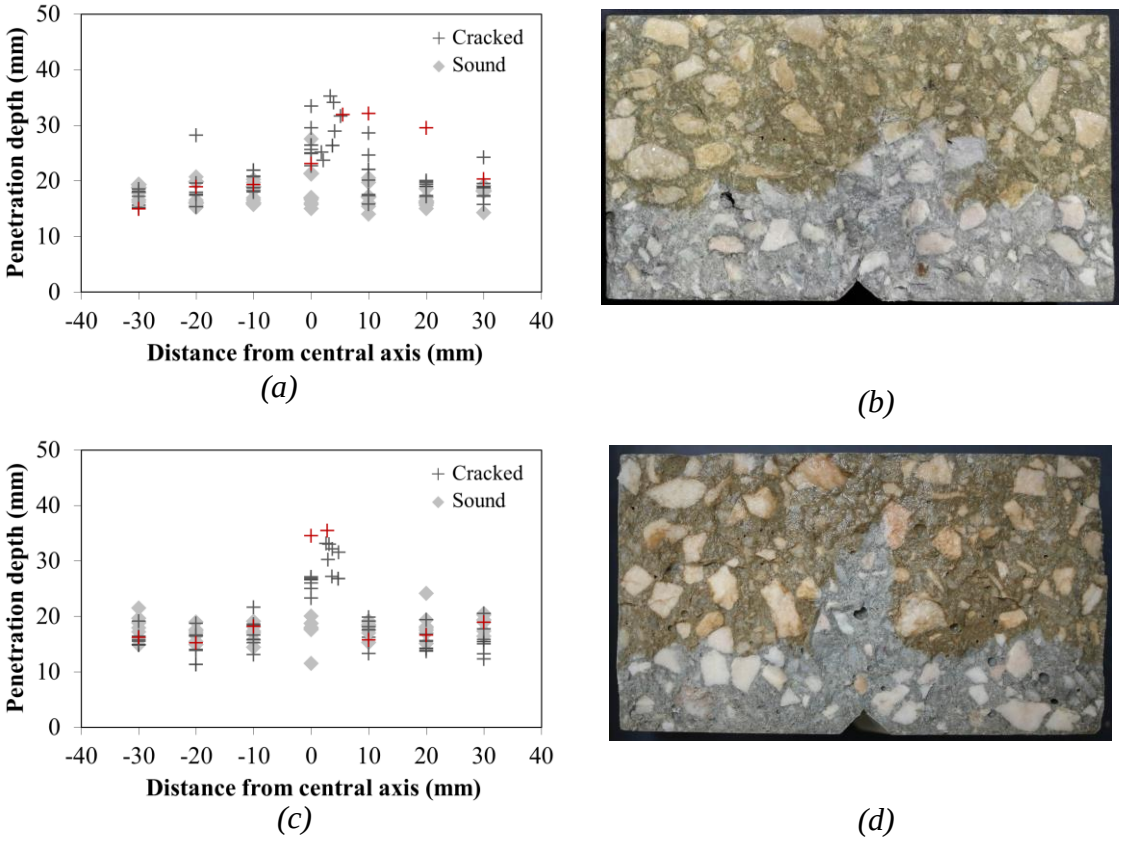

Figure 6. Chloride penetration depth for sound and cracked specimens of (a) OPC-7 and (c) OPC-28 concrete types (red profiles refer to the measurement surfaces shown in (b) and (d) respectively).

For sound specimens the penetration depth (x) was evaluated as the average penetration depth on the four splitting surfaces, obtaining a single value of D_{RCM} for each specimen (D_{sound}). For cracked specimens, however, it was not possible to evaluate a unique value of non-steady-state migration coefficient, since the penetration profile was very variable in the proximity of cracks. Hence, in this work, for each cracked specimens four different values of D_{RCM} were evaluated. In correspondence of the crack, the migration coefficient was evaluated considering the maximum penetration depth, averaged on the four different splitting surfaces (D_0). Moreover, D_{10}, D_{20} and D_{30} were evaluated, as the diffusion coefficient at ±10, ±20 and ±30 mm from the central symmetry axis, respectively, considering the penetration depths measured at these distances on the four splitting surfaces of each specimen.

Figure 7 shows the D_{RCM} obtained for the different cracked concretes, cured 7 and 28 days, while on side is reported the value of D_{sound}.

It can be observed that at 7 days of curing the concrete type showing highest values of D_{RCM} is the Pozzolanic one, having an average D_{sound} of 28.3×10^{-12} m^2/s, while for Portland-Limestone average D_{sound} was equal to 22.6×10^{-12} m^2/s and for Portland to 16.0×10^{-12} m^2/s. As expected, chloride migration coefficient decreases with curing time, and this can be seen comparing Figures 7a and 7b. This effect is particularly pronounced in the case of PC, where the average D_{sound} obtained at 28 days of curing is comparable to the value obtained for PLC, confirming that the refinement of pore microstructure in Pozzolanic cement requires prolonged curing times. Portland concrete resulted to have the lowest $D_{sound,}$ equal to 9.6×10^{-12} m^2/s after 28 days of moist curing.

In the 7-days cured cracked specimens it can be observed that the value of D_0 is significantly higher than the value of D_{sound} for all the tested concrete types. The effect is particularly pronounced for PLC-7, where D_0 reaches the value of 42.7×10^{-12} m^2/s in one specimen, around 90% higher than the average of D_{sound}. In correspondence of the crack, the values of D_0 were highly variable, depending on the geometrical parameters of crack, while moving away from the crack a similar decreasing trend was observed for all concrete types. In particular, D_{30} and D_{20} were comparable to $D_{sound,}$ while D_{10} showed values included between the value of D_0 and D_{20} for all the tested concrete types. This suggests that a crack may also affect the diffusion in transversal direction.

Similar considerations can be deduced for 28-day cured concretes, although the chloride penetration profile of PLC concrete type was only slightly affected by the presence of crack, but this is in accordance with results obtained on crack geometrical parameters (section 3.1).

In order to account for the effect of geometrical parameters of cracks, Figure 8a and 8b show the ratio between D_0 and D_{sound}, as function of crack width and crack depth, respectively. In this case, as D_0 values referred to the splitting surfaces where the crack geometrical parameters were analysed were taken into account, while for sound concrete the average D_{sound} was considered.

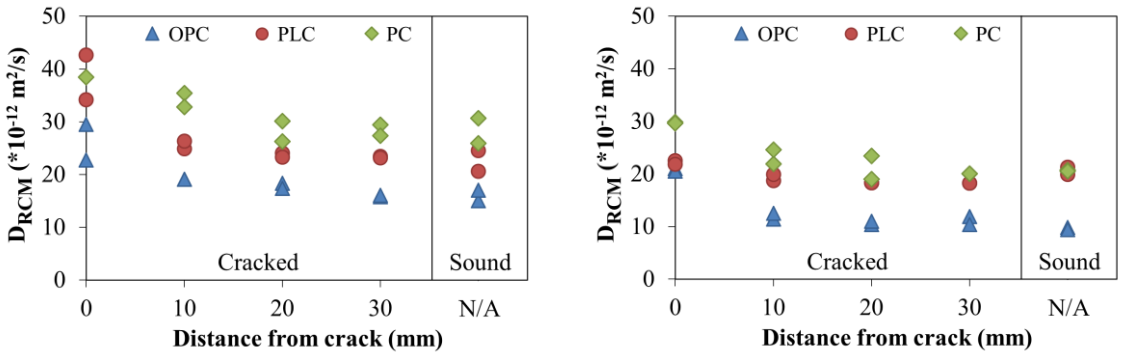

Figure 7. Non steady-state migration coefficient evaluated for the three concrete types after (a) 7 and (b) 28 days of curing.

Since with this cracking procedure it was not possible to establish a correlation between the obtained crack widths and crack depths, it was difficult to understand which one of the two parameter has most influence on the local increase of the migration coefficient. However, some preliminary observation can be inferred. As expected, the local increase of the migration coefficient resulted negligible for cracks characterized by both narrow widths (<15µm) and shallow depths (<5mm). For crack depths higher than 10 mm, the local increase became significant, with values of D_0/D_{sound} around 1.5 even in the case of narrow widths included in the range 10-20 µm. On the other hand, crack width was found to be the parameter that most affected the local increase in the migration coefficient when values were included in the range 35-50 µm. In these cases, in fact, the migration coefficient in correspondence of the crack resulted around 2 times higher than the migration coefficient in sound concrete, even when the crack depth was as shallow as 10 mm. Finally, ordinary Portland concrete, which previously showed an overall higher chloride penetration resistance, is the concrete type that showed the highest local increase in D_{RCM} in correspondence of crack, independently of curing time. These results show that micro-cracks influence the chloride migration coefficient also for crack widths below the critical threshold reported in literature, obtained with the same testing procedure on artificial cracks (Li *et al.*, 2016) or evaluated on load-induced cracks with other testing procedures (Jang *et al.*, 2011). On the other hand, results confirm the value of critical crack width reported in Yoon and Schlangen, 2014.

Further research will be done to assess the combined effect of crack width and crack depth on the local increase of chloride migration coefficient as well as an active load effect, which likely increase the crack width at the exposure surface.

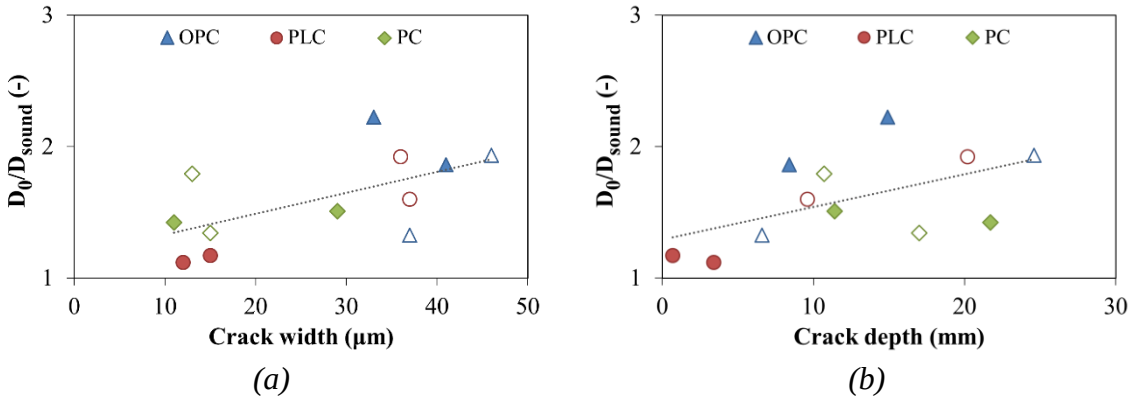

Figure 8. Relative increase of D_{RCM} in correspondence of cracks as function of (a) crack width and (b) crack depth (empty symbols represent7-day cured specimens, filled symbols 28-day cured specimens).

4 CONCLUSIONS

The chloride penetration resistance of concrete in uncracked condition and in presence of load-induced micro-cracks was evaluated for different concrete types. A specific specimen layout was developed, in order to enable the formation of bending-induced cracks. The cracking procedure resulted suitable to reproduce V-shaped micro-cracks with crack widths included in the range 10-50 µm and crack depth up to 25 mm. A slightly modified version of the so-called Rapid Chloride Migration test was successfully implemented, to evaluate the chloride penetration profile in correspondence of cracks. This enabled to evaluate the local variations of the chloride migration coefficient due to the presence of crack, as a function of two crack geometrical parameters, crack width and crack depth.

Pozzolanic concrete resulted the concrete type showing higher values of chloride migration coefficient in sound conditions, around 28.3×10^{-12} m^2/s, but it significantly decreased after 28 day of moist curing. Ordinary Portland concrete sowed lower values of migration coefficient in sound conditions both at 7 and 28 days of curing, with chloride migration coefficient resulting around 9.6×10^{-12} m^2/s after 28 days of moist curing.

The presence of micro-cracks had negligible effect on the value of chloride migration coefficient for cracks characterized by width lower than 15 μm and depth lower than 5 mm. For crack depth higher than 10 mm the migration coefficient in correspondence of crack resulted 1.5 times higher than in sound concrete, even for crack widths of 10-20 μm. For crack widths higher than 35-40 μm and crack depth higher than 10 mm the migration coefficient resulted to be doubled in correspondence of crack with respect to sound concrete.

REFERENCES

ACI Committee 318 (1999). *Building code requirement for structural Concrete.* American Concrete Institute.

Audenaert K., De Schutter G. and Marsavina L. (2007). The influence of cracks on chloride penetration in concrete structures - Part I: Experimental evaluation. In *Transport mechanisms in cracked concrete*, 35-43.

Bertolini L., Elsener B., Pedeferri P., Redaelli E. and Polder R. (2013). *Corrosion of steel in concrete: Prevention, diagnosis, repair (2nd ed.)*, Wiley VCH, Weinheim, Germany.

Djerbi, A., Bonnet, S., Khelidj A. and Baroghel-bouny V. (2008). Influence of traversing crack on chloride diffusion into concrete. *Cement and Concrete Research*, V.38, No.6, 877-883.

fib Bullettin 34 (2006). *Model code for service life design*.

Ismail M., Toumi A., Francois R. and Gagné R. (2008). Effect of crack opening on the local diffusion of chloride in cracked mortar samples. *Cement and Concrete Research*, V.38, No.8-9, 1106-1111.

Jang S.Y., Kim B.S. and Oh B.H. (2011). Effect of crack width on chloride diffusion coefficients of concrete by steady-state migration tests. *Cement and Concrete Research*, V.41, 9-19.

Li Y., Chen X., Jin L. and Zhang R. (2016). Experimental and numerical study on chloride transmission in cracked concrete. *Construction and Building Materials*, V.127, 425-435.

Marsavina L., Audenaert K., De Schutter G., Faur N. and Marsavina D. (2009). Experimental and numerical determination of the chloride penetration in cracked concrete. *Construction and Building Materials*, V.23, No.1, 264-274.

NT BUILD 492 (1999). *Concrete, mortar and cement-based repair materials: chloride migration coefficient from non-steady state migration experiments*. Nordtest, Espoo, Finland.

Park S.S., Kwon S.J., and Jung S.H. (2012). Analysis technique for chloride penetration in cracked concrete using equivalent diffusion and permeation. *Construction and Building Materials*, V.29, 183-192.

Şahmaran M. (2007). Effect of flexure induced transverse crack and self-healing on chloride diffusivity of reinforced mortar. *Journal of Materials Science*, V.42, No.22, 9131-9136.

Sosdean C., Marsavina L. and De Schutter G. (2016). Experimental and numerical determination of the chloride penetration in cracked mortar specimens. *European Journal of Environmental and Civil Engineering*, V.20, No.2, 231-249.

UNI EN 12390-3 (2003). *Testing Hardened Concrete - Compressive Strength of Test Specimens*.

Yoon I.S. and Schlangen E. (2014). Experimental examination on chloride penetration through micro-crack in concrete. *KSCE Journal of Civil Engineering*, V.18, No.1, 188-198.